THE ASTROPHYSICAL JOURNAL, 414:372–380, 1993 September 1

A TWO-REGION MODEL OF THE SOLAR WIND WITH COLLISIONLESS ELECTRON HEAT FLUX

P. ALEXANDER
Departamento de Fisica, Facultad de Ciencias Exactas y Naturales, Ciudad Universitaria, 1428 Buenos Aires, Argentina
Received 1992 October 6; accepted 1993 January 25

ABSTRACT

The present model divides the interplanetary space into an "inner region" and an "outer region." The solar wind is assumed to be one-fluid in the former zone and two-fluid in the latter zone, where a new equation for the electron heat flux replaces the classical heat conduction law because the plasma is not collision dominated. The model produces solutions for all physical quantities as functions of heliocentric distance that are in good agreement with quiet-time observations. The numerical results and a new interpretation of the gravitational potential energy show that the main energy conversions in the solar coronal expansion are from heat conduction and enthalpy into mechanical energy, whereas the magnetic component plays an insignificant role. It is also found that the total energy equation cannot be replaced by the polytropic law.

Subject heading: solar wind

1. INTRODUCTION

Various hydrodynamic models of the expansion of the solar coronal plasma into the surrounding interplanetary region have been developed since the original paper of Parker (1958). The significant differences among the equation sets arise from the treatment of the magnetic field and the expressions used for the energy equation and the closure relation.

After some years of measurements and theoretical studies it was realized that the solar wind could be considered to be one-fluid and thermally isotropic at short heliocentric distances, whereas far from the Sun the plasma becomes collisionless, which implies that the electrons and protons have different temperatures and that the protons become thermally anisotropic. Some models agreed on a two-region concept and estimated that the boundary between both zones should be conveniently chosen at 0.4 AU (e.g., Whang 1972; Acuña & Whang 1976).

The picture of a flow with classical, purely collisional heat conduction (Braginskii 1965; Spitzer 1962) for the whole heliosphere gave solutions that were qualitatively reasonable but quantitatively marginal. Many studies of the solar coronal expansion dealt with the breakdown of classical heat conduction (see, e.g., Forslund 1970; Hollweg 1976), and it has been argued that the behavior of solar wind electrons may be qualitatively different from what would be predicted from classical collisional transport theories (e.g., Scudder & Olbert 1983; Schoub 1988), at least for most of the heliosphere.

Chew, Goldberger, & Low (1956) considered the possibility of a macroscopic description for a collisionless plasma in a strong magnetic field and found a one-fluid equation set for the thermodynamic variables of the ions, that were coupled to the electrons only through the electromagnetic variables. This model has been widely used to describe interplanetary hydromagnetic phenomena (see, e.g., Scarf 1969; Burlaga & Turner 1976). The magnitude of the electromagnetic variables for a collisionless plasma in a strong magnetic field has been reexamined by Duhau (1984), and a two-fluid equation system in the limits in which the Larmor radius to mean free path ratio $\rightarrow 0$ (MHD approximation) and the electron-to-ion mass ratio $\rightarrow 0$ has been found from the moments of the Vlasov equation. It has been shown that the first-order electric field contributes to the equation of motion of ions (one of the assumptions underlying the CGL equations is that it can be assumed to be null) and electrons with a zero-order term, providing a coupling mechanism between the thermodynamic variables of both species. It is shown that the heat is mainly transported by the electrons, and it is considered, as suggested by the satellite data, that the electrons' thermal anisotropy is small, so that to a first approximation the heat transported by the ions and the anisotropy of the electrons may be neglected. To determine the electronic pressure it is necessary now to include the third-moment equatins of the electrons. The heat flux is parallel to the magnetic field according to observations in the solar wind, and the pressure tensors of both species are diagonal in a system that includes an axis in that direction (see, e.g., Feldman et al. 1975). This allows us to reduce the 27 components of the third-moment equations to only two independent ones, from which the corresponding macroscopic equations may be found provided that the velocity distribution function of the electrons is known. A simple mathematical representation of the measured quasi-stationary velocity distribution function of this species in the collisionless solar wind (Feldman et al. 1975) is used, and the electron energy equation and a closure relation, which could be called the electrons' collisionless heat flux law for the solar wind, are obtained. What gives rise to a heat flow is the fact that the electron population, as described by the velocity distribution function, breaks down into two distinct Maxwellian groups that possess, among others, different mean velocities. The model does not include the gravitational force of the Sun, but the alternative equation set that takes this field into account may be easily derived (see Alexander 1992).

A two-region model is applied in this paper to study the behavior of the magnetohydrodynamic variables that describe the solar coronal expansion. The same equations as Whang (1972) and Acuña & Whang (1976) are used for the inner region. An equation set found from the model for a collisionless plasma derived by Duhau (1984), that has already been used to study diverse phenomena occurring in the collision-free solar wind (see, e.g., Alexander & Duhau 1990), is used for the outer region. This leads to a replacement of the classical Spitzer-Härm law, employed for all heliocentric distances by all but a few models of the solar coronal

expansion incorporating an energy equation with heat conduction, by the collisionless heat flux equation in the outer region. Also notice that the collisionless model includes the two adiabatic CGL second-moment equations, while the other two papers used for the outer region the two general CGL equations, which include the ionic heat flux parallel and perpendicular to the interplanetary magnetic field. Two additional equations were needed to determine the parallel and perpendicular ionic heat flux, so these papers included the third-moment equations of Whang (1971).

A nonrotating spherical coordinate system (r, θ, ϕ) fixed to the center of the Sun is used to find the solutions of the two-region model for the equatorial plane of the Sun, where a steady state, axially symmetric flow is assumed to exist. The bulk velocity, the interplanetary magnetic field, and the heat flux all lie on that plane.

2. TWO-REGION MODEL

2.1. *Equation Set for the Inner Region*

The governing equations for the one-fluid inner region are

$$r^2 \rho U_r = C_m \,, \tag{1}$$

$$\frac{d}{dr}\left[r^2\left(\rho U_r^2 + P + \frac{B_\phi^2}{8\pi}\right)\right] - r\left(\rho U_\phi^2 + 2P - \frac{GM\rho}{r}\right) = 0 \,, \tag{2}$$

$$C_m r\left(U_\phi = \frac{B_\phi B_r}{4\pi\rho U_r}\right) = C_L \,, \tag{3}$$

$$C_m\left(\frac{U_r^2 + U_\phi^2}{2} + \frac{5P}{2\rho} + \frac{B_\phi^2}{4\pi\rho} - \frac{GM}{r} - \frac{U_\phi B_r B_\phi}{U_r 4\pi\rho}\right) + r^2 Q_r = C_E \,, \tag{4}$$

$$r^2 B_r = C_B \,, \tag{5}$$

$$r(U_r B_\phi - U_\phi B_r) = -\omega C_B \,, \tag{6}$$

$$Q_r = -k_0 T^{5/2} \frac{B_r^2}{B_r^2 + B_\phi^2} \frac{dT}{dr} \,, \tag{7}$$

$$Q_\phi = Q_r \frac{B_\phi}{B_r} \,, \tag{8}$$

$$P = \frac{2\rho k T}{m} \,, \tag{9}$$

where ρ is the mass density of the fluid, $\boldsymbol{U}$ the bulk velocity, P the isotropic pressure, $\boldsymbol{Q}$ the heat flux, $\boldsymbol{B}$ the interplanetary magnetic field, G the gravitational constant, M the mass of the Sun, m the proton mass, ω the angular speed of the Sun, k_0 the constant of thermal conductivity (of the order of 10^{-7} ergs cm^{-1} s^{-1} K$^{-7/2}$ for the solar wind), and k Boltzmann's constant, whereas C_m, C_L, C_E, and C_B are constants of motion (see, e.g., Alexander & Duhau 1992): the mass, angular momentum, energy, and magnetic fluxes. The above equations follow from the continuity equation, the radial and azimuthal components of the equation of motion, the energy equation, Gauss's law for the magnetic field, the Faraday-Henry law for a fluid with an infinite conductivity, the radial and azimuthal components of the classical heat condition law, and the last formula is the perfect gas law.

2.2. *Equation Set for the Outer Region*

The governing equations for the two-fluid outer region are equations (1), (5), (6), and (8) and the following expressions:

$$\frac{d}{dr}\left\{r^2\left[\rho U_r^2 + (P_\parallel - P_\perp)\frac{B_r^2}{B_r^2 + B_\phi^2} + P_\perp + P_e + \frac{B_\phi^2}{8\pi}\right]\right\} - r\left[\rho U_\phi^2 + (P_\parallel - P_\perp)\frac{B_\phi^2}{B_r^2 + B_\phi^2} + 2P_e + 2P_\perp - \frac{GM\rho}{r}\right] = 0 \,, \tag{10}$$

$$C_m r\left\{U_\phi - \frac{B_\phi B_r}{4\pi\rho U_r}\left[1 - \frac{P_\parallel - P_\perp}{(B_r^2 + B_\phi^2)/4\pi}\right]\right\} = C_L \,, \tag{11}$$

$$C_m \frac{P_\perp}{\rho(B_r^2 + B_\phi^2)^{1/2}} = C_{I1} \,, \tag{12}$$

$$C_m \frac{P_\parallel (B_r^2 + B_\phi^2)}{\rho^3} = C_{I2} \,, \tag{13}$$

$$C_m\left\{\frac{U_r^2 + U_\phi^2}{2} + \frac{5P_e}{2\rho} + \left(\frac{1}{2} + \frac{B_r^2}{B_r^2 + B_\phi^2}\right)\frac{P_\parallel}{\rho} + \left(1 + \frac{B_\phi^2}{B_r^2 + B_\phi^2}\right)\frac{P_\perp}{\rho} + \frac{B_\phi^2}{4\pi\rho} - \frac{GM}{r} - \left[1 - \frac{P_\parallel - P_\perp}{(B_r^2 + B_\phi^2)/4\pi}\right]\frac{U_\phi B_r B_\phi}{U_r 4\pi\rho}\right\} + r^2 Q_r = C_E \,, \tag{14}$$

$$Q_r = 2P_e U_r \left[\frac{(d/dr)\ln P_e}{(d/dr)\ln (B_r^2 + B_\phi^2)} - 1 \right], \tag{15}$$

where $P_\parallel$, $P_\perp$ refer to the proton pressure components that are parallel and perpendicular to the magnetic field and P_e to the isotropic electron pressure, whereas C_{I1} and C_{I2} are new constants of motion (see, e.g., Alexander & Duhau 1992): the first and second adiabatic invariants, the former being related to the invariance of magnetic moment of the protons (see Lynn 1967). Notice that equations (10), (11), and (14) reduce, respectively, to the one-fluid momentum and energy equations (2), (3), and (4) when $P_\parallel = P_\perp = P_e = P/2$, whereas equations (12) and (13) are the energy equations for the protons (CGL double adiabatic equations) and equation (15) is the new collisionless heat conduction law for the solar coronal expansion. The heat conduction is expressed as a factor times the convective heat flow $3/2P_e U_r$, the former being related to the variation of the electron pressure and the magnetic field. No total energy conservation for individual degree of freedom or for each species exists. Equations of state are not needed in this case to find the solutions of the equation set, but the temperature for each thermal component i may be found with $P_i = NkT_i$.

3. NUMERICAL SOLUTIONS

3.1. *Numerical Method*

In order to obtain numerical solutions both equations sets must be cast into the format

$$\begin{aligned} Y'_1 &= f_1(Y_1, Y_2, r) \\ Y'_2 &= f_2(Y'_1, Y_1, Y_2, r) \\ Y_3 &= f_3(Y'_1, Y'_2, Y_1, Y_2, r) \\ &\vdots \\ Y_N &= f_N(Y'_1, Y'_2, Y_1, \ldots, Y_{N-1}, r), \end{aligned}$$

where Y_j are the physical magnitudes, Y'_j their radial derivatives, and f_j are functions that do also depend on the constants of motion. The definitions for some dimensionless quantities used in the equations with the above structure are

$$\Gamma = \left(\frac{\omega r}{U_r}\right)^2, \quad \Delta = \frac{C_L}{C_m r^2 \omega}, \quad \Lambda = \frac{C_B^2}{4\pi C_m U_r r^2}.$$

For the inner region some manipulations lead to

$$\frac{dT}{dr} = \frac{C_m}{r^2 k_0 T^{5/2}} \left[1 + \Gamma \left(\frac{\Delta - 1}{1 - \Lambda} \right)^2 \right] \left\{ \frac{U_r^2}{2} \left[1 + \Gamma \left(\frac{\Delta - \Lambda}{1 - \Lambda} \right)^2 \right] + \frac{5kT}{m} + \omega^2 r^2 \Lambda \left(\frac{\Delta - 1}{1 - \Lambda} \right)^2 - \frac{GM}{r} - \omega^2 r^2 \Lambda \frac{(\Delta - 1)(\Delta - \Lambda)}{(1 - \Lambda)^2} - \frac{C_E}{C_m} \right\}, \tag{16}$$

$$\frac{dU_r}{dr} = \frac{U_r}{r} \frac{(4kt/m) - (2kr/m)(dT/dr) + 2\omega^2 r^2 \Lambda[(\Delta - 1)(\Delta - \Lambda)/(1 - \Lambda)^3] + \omega^2 r^2 [(\Delta - \Lambda)/(1 - \Lambda)]^2 - (GM/r)}{U_r^2 - (2kT/m) - \omega^2 r^2 \Lambda [\Delta - 1/(1 - \Lambda)^2]}, \tag{17}$$

$$\rho = \frac{C_m}{r^2 U_r}, \tag{18}$$

$$B_r = \frac{C_B}{r^2}, \tag{19}$$

$$U_\phi = \omega r \frac{\Delta - \Lambda}{1 - \Lambda}, \tag{20}$$

$$B_\phi = B_r \sqrt{\Gamma} \frac{\Delta - 1}{1 - \Lambda}, \tag{21}$$

that form a closed set with equations (7) and (8), whereas for the outer region the condition that $U_\phi \ll \omega r$, U_r and some transformations yield

$$\begin{aligned} \frac{dU_r}{dr} = \frac{U_r}{r} \Bigg\{ & (2 + \Gamma) \left[\frac{C_E}{C_m} - \frac{1}{2} U_r^2 - \omega^2 r^2 \Lambda \right] + \frac{2\Gamma}{(1 + \Gamma)^{1/2}} \frac{C_{I1} C_B}{C_m r^2} + \frac{(\Gamma + 6)(\Gamma - 1)}{2(1 + \Gamma)^2} \frac{C_{I2} C_m}{C_B^2 U_r^2} + \frac{GM}{r} \Bigg/ - \Gamma \left[\frac{C_E}{C_m} + \frac{GM}{r} \right] \\ & + (3\Gamma + 2) \frac{1}{2} U_r^2 - \omega^2 r^2 \Gamma - \frac{2\Gamma}{(1 + \Gamma)^{1/2}} \frac{C_{I1} C_B}{C_m r^2} + \frac{(\Gamma + 6)(\Gamma - 1)}{2(1 + \Gamma)^2} \frac{C_{I2} C_m}{c_B^2 U_r^2} \Bigg\}, \end{aligned} \tag{22}$$

$$\frac{dP_e}{dr} = -\frac{C_m}{r^3 U_r(1+\Gamma)}\left[2+\Gamma\left(1+\frac{r}{U_r}\frac{dU_r}{dr}\right)\right]\left[\frac{C_E}{C_m}-\frac{1}{2}U_r^2-\omega^2 r^2\Lambda-\frac{1+2\Gamma}{(1+\Gamma)^{1/2}}\frac{C_{I1}C_B}{C_m r^2}-\frac{3+\Gamma}{2(1+\Gamma)^2}\frac{C_{I2}C_m}{C_B^2 U_r^2}+\frac{GM}{r}\right], \quad (23)$$

$$P_\perp = \frac{C_{I1}\rho B_r(1+\Gamma)^{1/2}}{C_m}, \quad (24)$$

$$P_\parallel = \frac{C_{I2}\rho^3}{C_m B_r^2(1+\Gamma)}, \quad (25)$$

$$U_\phi = \omega r\left[\Delta-\Lambda+\frac{P_\parallel - P_\perp}{\rho U_r^2(1+\Gamma)}\right], \quad (26)$$

$$B_\phi = -B_r\sqrt{\Gamma}, \quad (27)$$

$$Q_r = \frac{1}{r^2}\left\{C_E - C_m\left[\frac{U_r^2}{2}+\frac{5P_e}{2\rho}+\left(\frac{1}{2}+\frac{1}{1+\Gamma}\right)\frac{P_\parallel}{\rho}+\left(1+\frac{\Gamma}{1+\Gamma}\right)\frac{P_\perp}{\rho}+\frac{B_\phi^2}{4\pi\rho}-\frac{GM}{r}\right]\right\}, \quad (28)$$

where equations (18) and (19) have to be inserted between equations (23) and (24), and equation (8) must be included at the end. Notice that both sets suit the desired format and that $Y_1 = T$ for the inner region and $Y_1 = P_e$ for the outer region, but $Y_2 = U_r$ for both zones.

Equation (17) has three points where a denominator vanishes. Each critical point occurs when the fluid velocity equals the characteristic propagation speed of a possible wave mode in the medium. The singular point closest to the Sun S_1 corresponds to the sonic point, and at the second and third singular points S_2 and S_3 the radial bulk velocity is equal to the radial and total Alfvén speeds, respectively. The solution for U_r must pass through all three singular points (for further details the reader is referred to Weber & Davis 1967 or Acuña & Whang 1976). No critical points exist at large heliocentric distances, but P_e must tend to 0 there.

The solutions depend upon eight parameters: the six constants of motion and the boundary conditions for Y_1 and Y_2 at some position. These parameters are not independent, because the constraints on U_r and P_e must be taken into account. Inward numerical integrations of equations (16) and (17) starting at S_3, where both the denominator and the numerator of (17) must vanish for U_r to remain continuous and dU_r/dr finite, will always pass through S_2 since both are near to each other and the latter is a node point. Both numerators and the denominator of equations (20) and (21) vanish at S_2, so that U_ϕ and B_ϕ remain finite and continuous at this point. At S_1, the numerator and denominator of equation (17) must again vanish simultaneously (or within a small fraction of the integration step at this position).

Given an initial set of values for the parameters consistent with measured solar wind conditions, the inward integration is started. This process is carried out several times, each time adjusting C_m, C_L, and r_3 or C_m, C_B, and r_3 until the numerator and denominator of equation (17) vanish at S_3 and also at S_1. Once the solution has successfully reached the Sun's surface, an outward integration starting at S_3 will provide a solution up to the transition point, where all quantities are continuous. The value of U_{r3} has to be adjusted in order to obtain a solution to equations (22) and (23) that satisfies $P_e \to 0$ at large distances. Again, the procedure is repeated several times, each time adjusting U_{r3}. The value of U_{r3} thus obtained is used to find new values of the parameters already adjusted for the inward integration as previously described, and then the equations are once more integrated in the outward direction to find a new value of U_{r3}. The iterative process is repeated enough times until the inner and outer solutions match across S_3 with 0.01% accuracy. Only three parameters remain completely independent as C_{I1} and C_{I2} must also be adjusted to ensure that $P_\parallel = P_\perp = P/2$ at the boundary between both regions. The numerical integrations are carried out by means of a fifth-order Runge-Kutta algorithm. Seven-digit accuracy is needed for some of the determined parameters to obtain a solution with the required conditions at the three critical points and at large distances.

3.2. *Results*

The different solutions that may be obtained with the above method are qualitatively similar. Two solutions are presented in this paper. The parameter values used in each case are listed in Table 1. They were selected as similar as possible to the values considered

TABLE 1

PARAMETER VALUES FOR SOLUTIONS 1 AND 2

Parameter	Solution 1	Solution 2
$C_m(10^{11}$ g s^{-1} sr$^{-1})$	0.8683246	1.032014
$C_L(10^{30}$ dyne cm sr$^{-1})$	0.8182725	0.9006493
$C_{I1}(10^{27}$ cm$^{5/2}$ g$^{1/2}$ s^{-2} sr$^{-1})$	4.26	4.14
$C_{I2}(10^{61}$ cm^7 s^{-5} sr$^{-1})$	2.22	1.58
$C_E(10^{25}$ ergs s^{-1} sr$^{-1})$	5.50	5.68
$C_B(10^{22}$ G cm^2 sr$^{-1})$	0.9790705	1.008990
$k_0(10^{-7}$ ergs cm^{-1} s^{-1} K$^{-7/2})$	1.88	1.81
$r_3(10^{12}$ cm)	1.825886	1.757191
$U_{r3}(10^7$ cm s$^{-1})$	2.729800	2.633799
$T_3(10^5$ K)	4.47	4.16

TABLE 2

NUMERICAL SOLUTION 1

r/r_s[a]	U_r (km s^{-1})	P (dyne cm^{-2})	P_e (dyne cm^{-2})	$P_{\|\|}$ (dyne cm^{-2})	$P_\perp$ (dyne cm^{-2})
1.00	2.11E+01	3.29E−03	...	...	...
1.78	6.30E+01	2.55E−04	...	...	...
3.65	1.31E+02	2.06E−05	...	...	...
7.24	1.92E+02	2.56E−06	...	...	...
13.9	2.38E+02	3.99E−07	...	...	...
29.3	2.79E+02	5.18E−08	...	...	...
53.6	3.02E+02	1.01E−08	...	...	...
86.2	3.17E+02	2.32E−09	1.16E−09	1.16E−09	1.16E−09
161	3.35E+07	...	1.98E−10	1.88E−10	1.10E−10
371	3.43E+07	...	2.25E−11	1.12E−11	6.64E−12
739	3.46E+07	...	3.08E−12	7.98E−13	7.66E−13
1509	3.48E+07	...	4.05E−13	4.80E−14	8.81E−14
2155	3.48E+07	...	1.33E−13	1.15E−14	2.99E−14

U_ϕ (km s^{-1})	N (cm^{-3})	B_r (γ)	B_ϕ (γ)	Q_r (ergs cm^{-2} s^{-1})	Q_ϕ (ergs cm^{-2} s^{-1})
1.88E+00	5.09E+06	2.02E+05	−1.51E+03	2.77E+04	−2.07E+02
2.80E+00	5.32E+05	6.32E+04	−8.41E+02	5.24E+03	−6.98E+01
3.89E+00	6.13E+04	1.51E+04	−4.09E+02	7.25E+02	−1.96E+01
4.61E+00	1.07E+04	3.86E+03	−2.03E+02	1.13E+02	−5.94E+00
4.70E+00	2.32E+03	1.04E−03	−1.03E+02	1.87E+01	−1.85E+00
4.29E+00	4.46E+02	2.34E+02	−4.66E+01	2.32E+00	−4.61E−01
3.14E+00	1.23E+02	7.02E+01	−2.46E+01	4.18E−01	−1.46E−01
2.40E+00	4.55E+01	2.72E+01	−1.48E+01	1.31E−01	−7.13E−02
2.13E+00	1.23E+01	7.79E+00	−7.62E+00	1.51E−02	−1.47E−02
8.89E−01	2.28E+00	1.48E+00	−3.23E+00	9.14E−04	−2.00E−03
3.94E−01	5.67E−01	3.70E−01	−1.60E+00	1.53E−04	−6.65E−04
1.90E−01	1.36E−01	8.92E−02	−7.85E−01	2.49E−05	−1.19E−04
1.33E−01	6.63E−02	4.35E−02	−5.47E−01	1.10E−05	−1.39E−04

[a] $215r_s = 1$ AU, where r_s indicates the solar radius.

TABLE 3

NUMERICAL SOLUTION 2

r/r_s	U_r (km s^{-1})	P (dyne cm^{-2})	P_e (dyne cm^{-2})	$P_{\|\|}$ (dyne cm^{-2})	$P_\perp$ (dyne cm^{-2})
1.00	2.37E+01	3.58E−03	...	...	...
2.04	7.83E+01	1.77E−04	...	...	...
4.53	1.47E+02	1.27E−05	...	...	...
7.21	1.89E+02	3.01E−06	...	...	...
14.3	2.36E+02	4.21E−07	...	...	...
28.7	2.69E+02	6.09E−08	...	...	...
52.9	2.90E+02	1.12E−08	...	...	...
86.2	3.04E+02	2.45E−09	1.23E−09	1.23E−09	1.23E−09
164	3.14E+02	...	2.37E−10	1.94E−10	1.16E−10
338	2.30E+02	...	4.05E−11	1.64E−11	1.02E−11
680	3.22E+02	...	5.77E−12	1.14E−12	1.14E−12
1397	3.23E+02	...	7.61E−13	6.61E−14	1.28E−13
2155	3.24E+02	...	1.74E−13	1.17E−14	3.46E−14

U_ϕ (km s^{-1})	N (cm^{-3})	B_r (γ)	B_ϕ (γ)	Q_r (ergs cm^{-2} s^{-1})	Q_ϕ (ergs cm^{-2} s^{-1})
1.85E+00	5.39E+06	2.08E+05	−1.61E+03	3.06E+04	−2.36E+02
2.92E+00	3.90E+05	4.99E+04	−7.85E+02	3.82E+03	−6.02E+01
4.14E+00	4.24E+04	1.02E+04	−3.51E+02	4.07E+02	−1.41E+01
4.37E+00	1.29E+04	4.00E+03	−2.18E+02	1.07E+02	−5.84E+00
4.28E+00	2.64E+03	1.02E+03	−1.07E+02	1.49E+01	−1.57E+00
3.82E+00	5.73E+02	2.52E+02	−5.12E+01	1.88E+00	−3.81E−01
2.82E+00	1.57E+02	7.44E+01	−2.68E+01	2.73E−01	−9.84E−02
2.11E+00	5.65E+01	2.80E+01	−1.60E+01	7.21E−02	−4.11E−02
1.75E+00	1.52E+01	7.82E+00	−8.26E+00	7.66E−03	−8.09E−03
7.88E−01	3.51E+00	1.83E+00	−3.93E+00	4.18E−04	−8.96E−04
3.39E−01	8.58E−01	4.51E−01	−1.94E+00	1.04E−04	−4.45E−04
1.62E−01	2.02E−01	1.07E−01	−9.38E−01	2.39E−05	−2.10E−04
1.06E−01	8.47E−02	4.48E−02	−6.07E−01	1.33E−05	−1.81E−04

TABLE 4

OBSERVED AND PREDICTED CONDITIONS AT 1 AU

VARIABLE	TYPICAL VALUE	Present Paper SOLUTION 1	Present Paper SOLUTION 2	ACUÑA & WHANG (1976) SOLUTION 1	ACUÑA & WHANG (1976) SOLUTION 2	WHANG 1972 SOLUTION
U_r (10^2 km s^{-1})	3.2	3.4	3.2	3.4	3.2	3.3
U_ϕ (km s^{-1})	8.0	1.7	1.4	1.7	1.4	...
N (cm^{-3})	8.0	6.8	8.7	5.8	7.3	5.5
T_e (10^5 K)	1.5	1.2	1.3	2.0	1.3	1.5
$T_\parallel$ (10^4 K)	6.6	7.9	6.6	12	9.4	12
$T_\perp$ (10^4 K)	3.3	4.2	3.7	6.9	6.4	5.3
Q (10^{-3} ergs cm^{-2} s^{-1})	5.0	5.6	3.8	11	4.3	4.9
B (γ)	5.0	7.1	7.6	7.2	7.7	6.3
Φ (degree)[a]	−53	−52	−54	−52	−57	−50

[a] Angle between the magnetic field and the radial direction.

by Acuña & Whang (1976) for two solutions, in order to compare both models. Detailed numerical results for the two solutions of this paper are given in Tables 2 & 3, whereas Table 4 exhibits some average properties of the low-speed solar wind at 1 AU and the values predicted by the present model at this position. The quantities show generally good agreement with observations. Table 4 also includes the results at 1 AU of the two-region models by Whang (1972) and Acuña & Whang (1976). Notice that the present model leads to predictions of parallel and perpendicular proton temperatures that are much closer to the observed values at 1 AU. Graphs are shown for solution 1.

The profiles obtained for U_r and U_ϕ, which are similar to those presented by previous models, are shown in Figure 1. The solution for U_r passes without problems through all critical points. A smooth behavior for U_ϕ at 0.4 AU would probably represent the more likely physical situation rather than the abrupt transition found by the model.

The pressure components $P/2$ (if P was represented the curve would not be continuous), P_e, $P_\parallel$, and $P_\perp$ are given in Figure 2. All of them tend to zero for large distances. Notice the remarkable decrease in the order of magnitude of the pressure for increasing heliocentric distances.

The number density N, where $N = \rho/m$, is shown in Figure 3. At short distances N falls off rapidly because there is a steep rise of U_r and for large distances $N \propto r^{-2}$ because U_r stays almost constant.

Figure 4 exhibits the evolution of B_r and B_ϕ and Figure 5 of Q_r and Q_ϕ. The magnetic field and the heat flux are dominated by the radial component near the Sun and by the azimuthal component at large distances, whereas at 1 AU the two components are nearly the same for both quantities. The collisionless heat flux profile in the outer region is different from the one obtained with classical heat conduction (compare it, e.g., with the solution in Whang 1972).

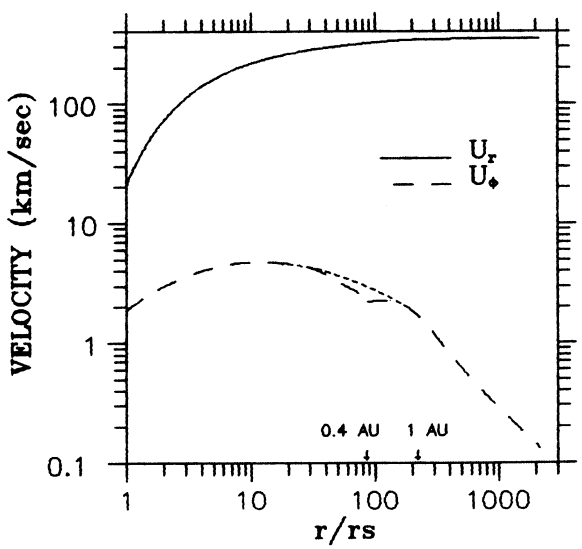

FIG. 1

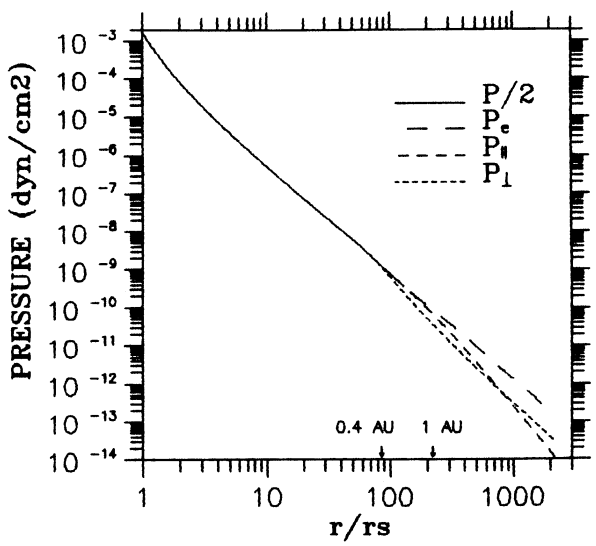

FIG. 2

FIG. 1.—Radial and azimuthal velocities as functions of heliocentric distance. The dotted line represents a probable physical situation for the azimuthal velocity near the boundary between the inner and the outer regions.

FIG. 2.—Electron pressure, and parallel and perpendicular proton pressures as functions of heliocentric distance

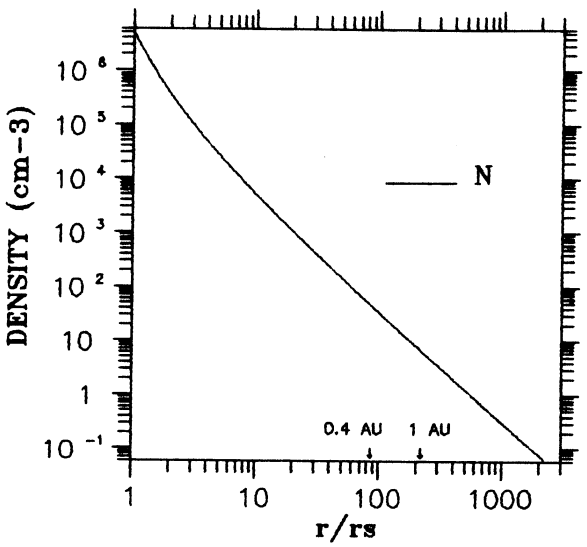

FIG. 3

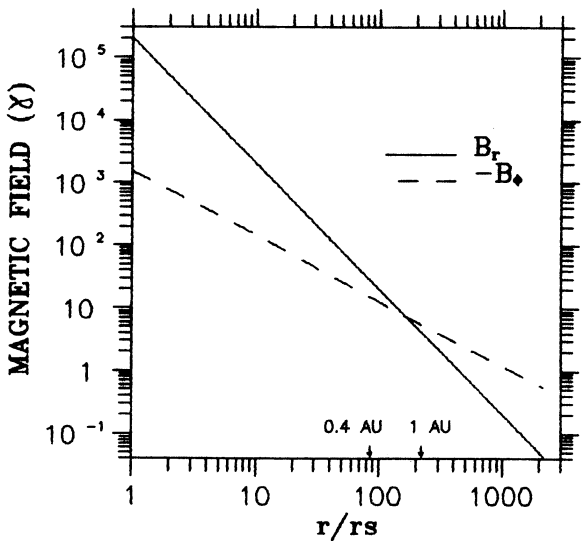

FIG. 4

FIG. 3.—Electron or proton number density as a function of heliocentric distance
FIG. 4.—Radial and azimuthal magnetic fields as functions of heliocentric distance

4. INTERPRETATIONS AND DISCUSSIONS OF RESULTS

The flux of the diverse energy forms along the solar coronal expansion are studied below. The following terms are defined to accomplish this task:

$$E_k = \tfrac{1}{2} C_m (U_r^2 + U_\phi^2) ,$$

$$E_t^c = \tfrac{5}{2} P U_r r^2 ,$$

$$E_t^{cl} = \left[\frac{5}{2} P_e + P_\parallel \left(\frac{1}{2} + \frac{B_r^2}{B_r^2 + B_\phi^2} \right) + P_\perp \left(1 + \frac{B_\phi^2}{B_r^2 + B_\phi^2} \right) \right] U_r r^2 + (P_{\parallel - P_\perp}) \frac{B_r B_\phi}{B_r^2 + B_\phi^2} U_\phi r^2 ,$$

$$E_m = \frac{(B_\phi U_r - B_r U_\phi) B_\phi r^2}{4\pi} ,$$

$$E_h = r^2 Q_r ,$$

$$E_g = - \frac{GMC_m}{r} + E_{go} .$$

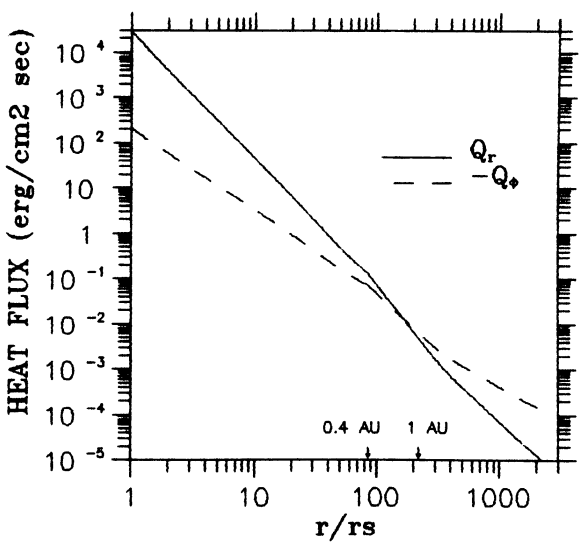

FIG. 5.—Radial and azimuthal heat fluxes as functions of heliocentric distance

In these expressions E_k, E_t^c, E_t^{cl}, E_m, E_h, and E_g represent, respectively, the following energy fluxes per unit time per unit steradian: kinetic, thermal (enthalpy) collisional and collisionless (E_t^{cl} reduces to E_t^c for $P_e = P_\parallel = P_\perp = P/2$), magnetic field, heat, and gravitational potential. Notice that E_{g_0} is an arbitrary constant (only differences in potential energy matter) that may be chosen so that E_g vanishes on the Sun's surface, which then allows us to interpret this term as the work spent against gravity to transport the plasma from that position into space.

As $E_k + E_t + E_m + E_h + E_g = C_E + E_{g_0}$ the fractional energy flux ϵ_i for the ith form of energy is given by

$$\epsilon_i = \frac{E_i}{C_E + E_{g_0}} .$$

These ratios have been plotted in Figure 6. The logarithmic scale on the vertical axis makes it difficult to visualize that the sum of all fractions is uniformly 1.

The spiral magnetic field inhibits heat conduction in the radial direction, thus reducing that energy flow and increasing the efficiency with which it is converted into other forms of energy as the heliocentric distance increases. The magnetic field energy flux is a monotonic decreasing function of the heliocentric distance, and it amounts to only about 1% of the total energy flux. The curves also show that the solar coronal expansion transforms energy of thermal origin (99% of the total energy near the Sun's surface), mainly heat, into mechanical energy (99% of the total energy at large distances), mainly gravitational potential. It may be also observed that the main energy conversions happen in the collisional region and that the relative contribution of each component is exactly inverted along the whole process.

As shown in Figure 7, in the outer region the ratio of the proton pressure $P_p = (P_\parallel + 2P_\perp)/3$ and P_e decreases monotonically. The ratio of $P_\parallel$ to $P_\perp$ increases rapidly with increasing heliocentric distance reaching a maximum value of 1.7 near 1 AU and then decreases monotonically and becomes less than unity for large heliocentric distances. The very low collision frequency in the outer region ensures that each pressure component does not strongly affect the others. When instability criteria were tested on both solutions, neither the fire-hose nor the mirror instabilities were expected to occur.

Some one-fluid solar wind models have considered a polytrope index to describe the relation between P and N (see, e.g., Weber & Davis 1967), and some two-fluid models tested such an index for the relation between P_e and N (see, e.g., Whang 1972). For the inner and outer regions the polytrope index γ may be defined, respectively, as

$$\gamma = \frac{N}{P}\frac{dP/dr}{dN/dr},$$

$$\gamma = \frac{N}{P_e}\frac{dP_e/dr}{dN/dr} .$$

The polytrope index as a function of heliocentric distance can be calculated from the present solutions, and the result is also plotted in Figure 7. The index asymptotically approaches 5/3, the adiabatic value, for large distances. The large variation of γ indicates that the polytropic law, which assumes that the index is constant throughout the whole region, cannot replace the energy equation.

According to the values that have been computed for the lower heliocentric distances the angular momentum loss of the Sun is caused in 99.9% by the torque that the interplanetary magnetic field exerts on the Sun, only 0.01% is related to the azimuthal

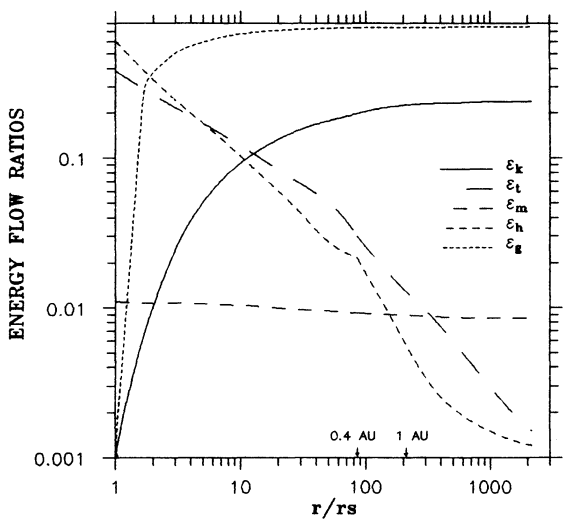

FIG. 6

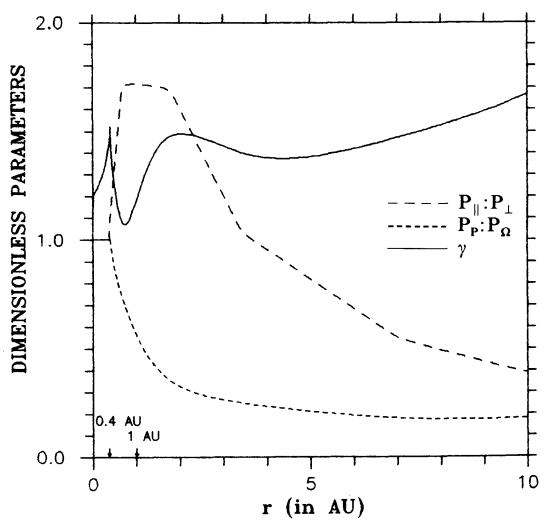

FIG. 7

FIG. 6.—Kinetic, thermal, magnetic field, heat, and gravitational potential energies to total energy ratios as functions of heliocentric distance
FIG. 7.—Proton pressure anisotropy ratio, the proton to electron pressure ratio, and the polytropic index as functions of heliocentric distance

velocity of the plasma. This fact shows that the magnetic field plays a much more significant role for the angular momentum than for the energy, at least near the Sun.

In this model, coronal quantities do not enter as boundary conditions but are inferred from the values of the chosen parameters as the integration proceeds to the Sun's surface. Temperatures of the order of 2×10^6 K are found for the lower corona with this model, in agreement with observations.

REFERENCES

Acuña, M., & Whang, Y. C. 1976, ApJ, 203, 720
Alexander, P. 1992, Ph.D. thesis, Univ. Buenos Aires
Alexander, P., & Duhau, S. 1990, J. Geophys. Res., 95, 19149
———. 1992, Rev. Brasileira Geofis., 10, 19
Braginskii, S. I. 1965, Rev. Plasma Phys. Vol. 1, (New York: Consultants Bureau)
Burlaga, L. F., & Turner, J. M. 1976, J. Geophys. Res., 81, 73
Chew, G. F., Goldberger, M. L., & Low, F. E. 1956, Proc. Roy. Soc. Lond. A236, 112
Duhau, S. 1984, J. Plasma Phys., 32, 23
Feldman, W. C., Asbridge, J. R., Bame, S. J., Montgomery, M. D., & Gary, S. P. 1975, J. Geophys. Res., 80, 4181
Forslund, D. W. 1970, J. Geophys. Res., 75, 17
Hollweg, J. V. 1976, J. Geophys Res., 81, 1649
Lynn, Y. M. 1967, Phys. Fluids, 10, 2278
Parker, E. N. 1958, ApJ, 128, 664
Scarf, F. L. 1969, Space Sci., 17, 505
Schoub, E. C. 1988, in Proc. 6th Internat. Solar Wind Conf., ed. V. J. Pizzo et al. (Boulder: National Center for Atmospheric Research), 59
Scudder, J. D., & Olbert, S. 1983, in Solar Wind Five, ed. M. Neugebauer (NASA CP 2280), 163
Spitzer, L. 1962, Physics of Fully Ionized Gases (New York: Interscience)
Weber, E. J., & Davis, L. 1967, ApJ, 148, 217
Whang, Y. C. 1971, J. Geophys. Res., 76, 7503
———. 1972, ApJ, 178, 221